Available online at www.sciencedirect.com

SCIENCE DIRECT®

Applied Surface Science 212–213 (2003) 428–432

applied surface science

www.elsevier.com/locate/apsusc

Time-resolved photoluminescence study of excitons in thin PTCDA films at various temperatures

A.Yu. Kobitski[a,*], R. Scholz[a], G. Salvan[a], T.U. Kampen[a], H.P. Wagner[b], D.R.T. Zahn[a]

[a]*Institut für Physik, Technische Universität Chemnitz, D-09107 Chemnitz, Germany*
[b]*Department of Physics, University of Cincinnati, Cincinnati, OH 45221-0011, USA*

Abstract

In the present work excitons in thin 3,4,9,10-perylene tetracarboxylic dianhydride (PTCDA) films are studied by means of time-resolved photoluminescence (TRPL) in the temperature range from 10 to 300 K. The obtained temperature dependence of different recombination channels, arising from an indirect minimum of the Frenkel exciton dispersion, different types of self-trapped excitons and relaxed excited monomer states, are compared to the corresponding PL recombination channels for single crystals. The Frenkel excitons (FEs), the slow PL channel, the excimer decay times, and the PL intensities reveal a similar temperature dependence like in the single crystals, while the contribution of the charge-transfer exciton (CTE) is twice as large in films.

PACS: 71.35.Aa; 73.20.At; 78.55.Kz

Keywords: PTCDA; Time-resolved photoluminescence; Frenkel excitons; Self-trapped excitons

---

1. Introduction

In the last few years, 3,4,9,10-perylene tetracarboxylic dianhydride (PTCDA) is one of the most intensively investigated prototypic molecules forming well-ordered polycrystalline films on a variety of substrates [1]. In spite of various spectroscopic and electronic studies a clear picture of the electronic band structure is still under debate. Recently, a model of absorption, relaxation and recombination processes of excitons in PTCDA single crystals was developed based on the results of time-resolved photoluminescence (TRPL) measurements at different temperatures [2–4], giving evidence for PL arising from Frenkel excitons (FEs), charge-transfer excitons (CTE), excimer states, and a further recombination channel called slow (S)-band in the following. The origin of the S-band decaying with a characteristic time of $\tau_s = 40$ ns at 10 K is still not known, while the other experimental findings were supplemented by quantum chemical calculations based on the approach of the transfer of Frenkel excitons, including a realistic three-dimensional crystal structure with two molecules per unit cell [5,6] and calculations of different PTCDA dimer geometries with time-dependent density functional theory [4,7,8].

---

[*] Corresponding author. Present address: Department of Biophysics, University of Ulm, Albert-Einstein-Allee 11, D-89069 Ulm, Germany. Tel.: +49-731-50-23042; fax: +49-731-50-23059.
E-mail address: andrei.kobitski@physik.uni-ulm.de
(A.Yu. Kobitski).

0169-4332/03/$ – see front matter © 2003 Elsevier Science B.V. All rights reserved.
doi:10.1016/S0169-4332(03)00126-0

In this paper, we apply the developed models to the characterization of thin PTCDA films on Si(1 0 0) by means of TRPL measurements at various temperatures. The obtained model parameters are compared to the corresponding values for the single crystal.

2. Experimental

The PTCDA sublimation and film deposition were described elsewhere [9,10]. Briefly, the 40 nm PTCDA films studied here were grown by organic molecular beam deposition (OMBD) on hydrogen-passivated p-type (0 0 1)-oriented Si at 410 K substrate temperature. By fixing the temperature of the Knudsen cell at $T = 550$ K the evaporation rate of the PTCDA source material was kept of about 0.3 nm/min. For the time-resolved PL measurements, the PTCDA films were excited with a pulsed dye laser synchronously pumped by a mode-locked Ar^+ ion laser, resulting in 20 ps pulses at an energy of 2.19 eV (565 nm) and in a laser spot of about 250 μm focused on the sample. The intrinsic repetition rate of 80 MHz defined by the cavity length of the ion laser was reduced to 4 MHz using a cavity dumper. The time-resolved PL was analysed using a CROMEX 250IS imaging spectrograph and detected by a Hamamatsu C4334 Streakscope with a time resolution better than 50 ps. In order to protect the streakscope against stray light from the laser, a filter with a cutoff at 570 nm (2.18 eV) was used. In the range 1.5–2.1 eV investigated in the present work, the flatness of the spectral response of the entire measuring system was checked with black body radiation from a tungsten lamp with known emission spectrum, and therefore no spectral correction was applied to the subsequent PL measurements. For the low temperature ($T = 10$–300 K) measurements, a closed-cycle He cryostat CTI-Cryogenics was used.

3. Results and discussion

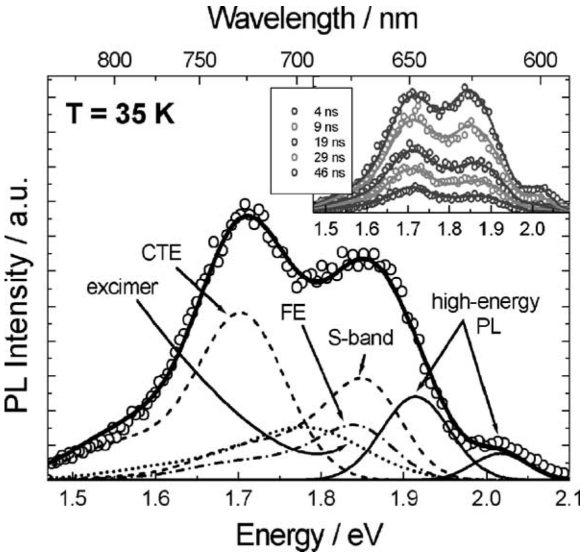

Fig. 1. The time-integrated PL spectrum measured at 35 K is shown as open circles. The contribution of CTE (dashed), excimer (dotted), S-band (dashed), Frenkel exciton (FE) (dash–dotted), and two high-energy PL bands (solid) with peak positions at 1.70, 1.78, 1.83, 1.84, 1.91, and 2.02 eV, respectively, are shown separately. The inset shows the PL spectra (circles) measured at different delay times after the excitation pulse (4, 9, 19, 29, and 46 ns) together with the simulated spectra (solid lines) constructed as the sum of all PL components taken with exponentially time-dependent prefactors.

In Fig. 1 we show the line-shapes of the Frenkel exciton, S-band, charge-transfer exciton, excimer and monomer components and their relative contribution to the PL spectrum measured at 35 K. As a model function for the line-shapes we used a sum of normalized Gaussians with positions ω_j, broadenings σ_j and areas a_j:

$$I_{\mathrm{PL}}(\hbar\omega) = \omega^3 \sum_j \frac{a_j}{\sigma_j\sqrt{2\pi}} \exp\left(-\frac{1}{2}\left(\frac{\omega-\omega_j}{\sigma_j}\right)^2\right), \tag{1}$$

where the multiplicative factor ω^3 is related to the density of states of the emitted photons [11]. By performing a simultaneous fit of the PL spectra taken at different delay times and at different temperatures, a temperature blueshift of the CTE peak position by 15×10^{-2} meV/K was obtained. The peak positions of the vibronic bands at 0 K were fitted to be at 1.695 and 1.555 eV. Their broadenings and the area ratio were kept constant with FWHM values of 125 and 160 meV for the first and second vibronic bands, respectively, and 0.4 for the area ratio. The peak positions, broadenings and area ratios for the excimer vibronic bands were kept constant with values of 1.78 and 1.63 eV for the peak positions, 165 and 200 meV for their broadenings, and 0.5 for the area ratio. The parameters for the Frenkel exciton were kept the same as for the single crystal [3] except for a slightly larger broadening of the first vibronic band, e.g. peak positions at 1.83, 1.68, and 1.53 eV at 0 K and a linear slope of about 5×10^{-2} meV/K for their temperature dependence, 0.4 for the vibronic areas ratio, and broadenings modelled according to [7]:

$$\sigma_j^2 = \Delta E^2 = \sigma_{0j}^2 + \alpha_{\text{int}}^2 (\hbar\omega_{\text{int}})^2 \coth\left(\frac{\hbar\omega_{\text{int}}}{2k_{\text{B}}T}\right) + \alpha_{\text{ext}}^2 (\hbar\omega_{\text{ext}})^2 \coth\left(\frac{\hbar\omega_{\text{ext}}}{2k_{\text{B}}T}\right), \qquad (2)$$

where the σ_0 values were adjusted to 70, 85, 90, 100, and 120 meV based on the fit of the low temperature spectra, the values of $\alpha_{\text{int}}^2 = 0.29$, $\omega_{\text{int}} = 233\ \text{cm}^{-1}$ are taken from [12], and the values of $\alpha_{\text{ext}}^2 = 7.5$, and $\omega_{\text{ext}} = 50\ \text{cm}^{-1}$ are extracted from Raman measurements [7,9]. The parameters for the S-band were the same as for the Frenkel exciton, except for the slightly higher peak positions of the vibronic bands at 1.84 and 1.69 eV at 0 K. The high-energy PL bands attributed to the recombination from monomer or surface states were fitted with a single Gaussian function positioned at 1.92 and 2.01 eV, respectively, with a FWHM of about 100 meV.

In the next step, the decay times $\tau(T)$ and PL intensities $I_{\text{PL}}(T)$ of all components were extracted for different temperatures. In Fig. 2, the dependence is shown for the Frenkel exciton, S-band, CTE and excimer together with the fitting curves according to [13]:

$$\frac{1}{\tau(T)} = \frac{1}{\tau_{\text{rad}}} + \sum_j \gamma_j^{\text{nrad}} \exp\left(-\frac{\Delta_j^{\text{nrad}}}{k_{\text{B}}T}\right), \qquad (3)$$

and

$$I_{\text{PL}}(T) = I_0 \exp\left(-\frac{\vartheta}{k_{\text{B}}T}\right)\frac{\tau(T)}{\tau_{\text{rad}}}, \qquad (4)$$

where τ_{rad} is the radiative decay time for the state of interest, k_{B} the Boltzmann's constant, and γ_j^{nrad} and Δ_j^{nrad} the rate and the activation energy of the non-radiative process, respectively, I_0 is proportional to the density of excitons in the initial states after optical excitation, and ϑ the barrier between the initial states after optical excitation and the emissive states.

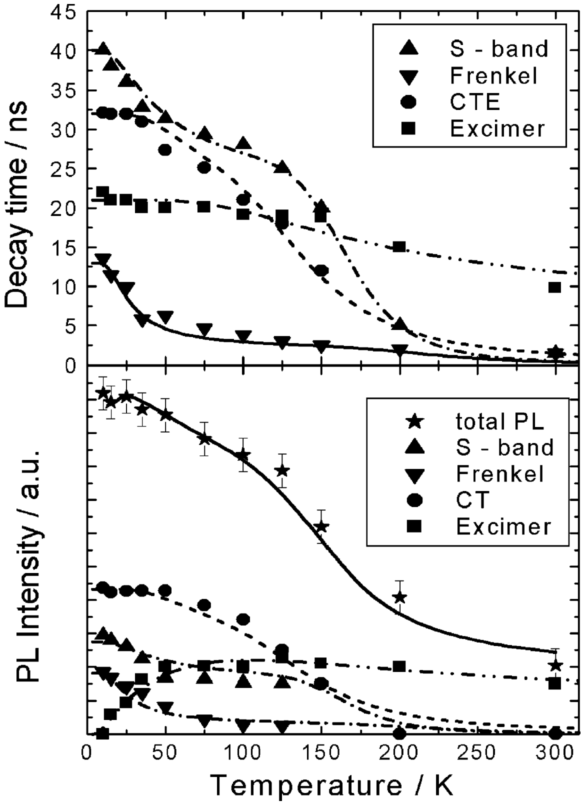

Fig. 2. Extracted PL decay times (upper) and intensities (lower) of the S-band (up triangles), Frenkel excitons (down triangles), CTE (circles) and excimer states (squares) are shown as a function of temperature (symbols) together with the fitted curves (lines). The experimental (stars) and simulated total intensity (solid line) is calculated as the sum of all PL intensities shown.

In all cases except for the excimer PL, where a barrier of about 2.5 meV between the precursor and the excimer state was obtained, the temperature dependence of the PL intensities were just proportional to the decay times, i.e. the barriers ϑ were close to zero. The temperature dependence of the excimer decay time is described by a radiative recombination with a lifetime of 21 ns and by a thermally activated non-radiative escape over a barrier of 30 meV. For the Frenkel exciton and the S-band, the recombination dynamics is described at low temperatures as in the case of a single crystal with radiative lifetimes of 13 and 40 ns, respectively [2]. At higher temperatures, we observe two non-radiative decay channels involving activation energies of 135 and 5.5 meV, where the latter was attributed to the trapping barrier into the

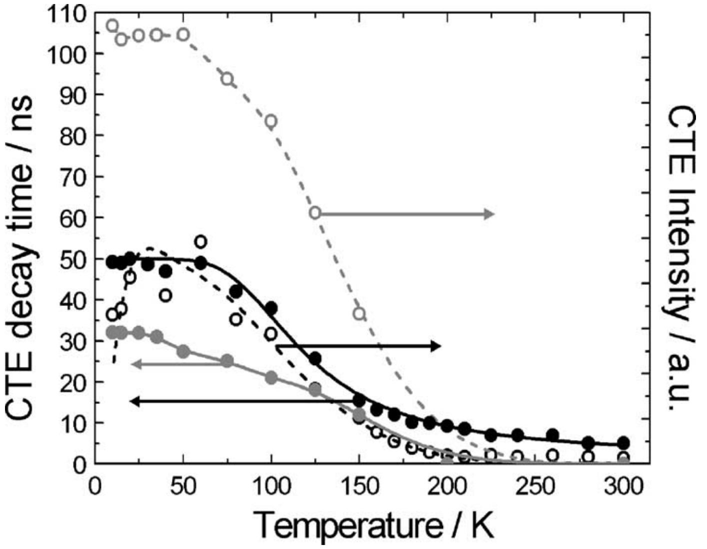

Fig. 3. The temperature dependence of the PL decay times (filled circles) and intensities (open circles) of the CTE for single crystals (black) and films (grey) are shown together for comparison.

CTE states. The temperature dependence of the excimer, Frenkel exciton and S-band channels in thin films is similar to that observed for single crystals, while the CTE recombination dynamics, i.e. the decay times and the PL intensities, differs. A comparison between the temperature dependence of the decay times and the PL intensities of the single crystals and films are shown in Fig. 3, where the CTE intensities are plotted relative to the normalised excimer intensities for crystals and films. The CTE contribution to the total PL intensity is less than 20% in the crystals and 40% in the films, respectively. The lifetime at low temperatures is about 32 ns, somewhat faster than the corresponding lifetime of about 53 ns in single crystals. Also, the non-radiative PL quenching occurs over barriers of 14 and 73 meV, while for single crystals only a single barrier of about 40 meV is observed. The differences in the CTE kinetics of single crystals and films can be assigned to the presence of another type of self-trapped exciton in films with faster decay time populated directly by scattering processes out of the optically excited state.

The high-energy bands at 1.92 and 2.01 are probably related to the recombination from the relaxed Frenkel exciton state at the edge of the Brillouin zone accompanied by an emission of external vibrations (phonons) and low-frequency internal breathing modes or from surface states. Furthermore, the cutoff filter at 2.10 eV could influence on details of the shape of the highest energy band. In any case, their summed contribution does not exceed 1% of the total PL intensity.

4. Summary

In conclusion, time-resolved photoluminescence spectra of thin PTCDA films have been measured in the temperature range from 10 to 300 K. Various types of excitons like Frenkel excitons, self-trapped excitons and monomers were observed. The excimer, S-band and Frenkel exciton PL channels show a temperature dependence of the decay time and PL intensity similar to single crystals, while the charge-transfer exciton contribution is larger and the corresponding decay time faster. We suggest that this observation can be assigned to the presence of a further self-trapped exciton state.

Note added

In Refs. [3,8], the PL channel called S-band in the present manuscript was assigned to a charge transfer exciton involving both molecules in the crystal unit cell.

Acknowledgements

The authors gratefully acknowledge the Graduiertenkolleg "Dünne Schichten und nichtkristalline Materialien" at the Technical University of Chemnitz, and the EU funded Human Potential Research Training Network DIODE (Contract No.: HPRN-CT-1999-00164) for financial support.

References

[1] S.R. Forrest, Chem. Rev. 97 (1997) 1793.
[2] A.Yu. Kobitski, R. Scholz, I. Vragovic, H.P. Wagner, D.R.T. Zahn, Phys. Rev. B 66 (2002) 153204.
[3] A.Yu. Kobitski, R. Scholz, H.P. Wagner, D.R.T. Zahn, Phys. Rev. B (2003), submitted for publication.
[4] A.Yu. Kobitski, Ph.D. Thesis, Chemnitz (2003).
[5] I. Vragovic, R. Scholz, M. Schreiber, Europhys. Lett. 57 (2002) 288.
[6] R. Scholz, I. Vragovic, A.Yu. Kobitski, M. Schreiber, H.P. Wagner, D.R.T. Zahn, Phys. Stat. Sol. B 234 (2002) 402.
[7] R. Scholz, I. Vragovic, A.Yu. Kobitski, G. Salvan, T.U. Kampen, M. Schreiber, D.R.T. Zahn, in: V.M. Agranovich, G.C. La Rocca (Ed.), Proceedings of Course CXLIX: Organic Semiconductors: Science and Application, International School of Physics "E. Fermi", IOS Press, Amsterdam, 2002, pp. 379–403.
[8] R. Scholz, A.Yu. Kobitski, I. Vragovic, T.U. Kampen, D.R.T. Zahn, H.-P. Wagner, in: Proceedings of the 26th International Conference on the Physics of Semiconductors, 2002, in press.
[9] G. Salvan, D.A. Tenne, A. Das, T.U. Kampen, D.R.T. Zahn, Org. Electron. 1 (2000) 49.
[10] A.Yu. Kobitski, G. Salvan, H.P. Wagner, D.R.T. Zahn, Appl. Surf. Sci. 179 (2001) 209.
[11] R. Loudon, The Quantum Theory of Light, Clarendon Press, Oxford, 1983 (Chapter 2.4).
[12] R. Scholz, A.Yu. Kobitski, T.U. Kampen, M. Schreiber, D.R.T. Zahn, G. Jungnickel, M. Sternbrg, Th. Frauenheim, Phys. Rev. B 61 (2000) 13659.
[13] N.J. Turro, Modern Molecular Photochemistry, University Science Book, Mill Valley, CA, 1991 (Chapter 5.7).